Microwave-Assisted Green Synthesis of Silver Nanoparticles Using Orange Peel Extract

ARTICLE *in* ACS SUSTAINABLE CHEMISTRY & ENGINEERING · NOVEMBER 2013

Impact Factor: 4.64 · DOI: 10.1021/sc4003664

ACS Sustainable Chemistry & Engineering

Research Article

pubs.acs.org/journal/ascecg

Microwave-Assisted Green Synthesis of Silver Nanoparticles Using Orange Peel Extract

Genevieve A. Kahrilas,[†,§] Laura M. Wally,[‡] Sarah J. Fredrick,[‡] Michael Hiskey,[†] Amy L. Prieto,[‡] and Janel E. Owens*[,†]

[†]Department of Chemistry and Biochemistry, University of Colorado, Colorado Springs, 1420 Austin Bluffs Parkway, Colorado Springs, Colorado 80918, United States

[‡]Department of Chemistry, Colorado State University, Ft. Collins, Colorado 80523, United States

Supporting Information

ABSTRACT: Silver nanoparticles (AgNPs) were prepared in a one-step microwave-assisted synthesis guided by the principles of green chemistry. Microwave parameters were optimized using the Box–Benhken design for three factors (time, temperature, and pressure). Aqueous extracts from the peels of citrus fruits (orange, grapefruit, tangelo, lemon, and lime) were used for the synthesis of AgNPs using microwave technology, though the synthesis of AgNPs was only successful using the orange peel extract. Nanospheres of TEM mean diameter (with standard deviation) of 7.36 ± 8.06 nm were successfully synthesized in 15 min by reducing Ag^+ ions (from $AgNO_3$) with orange peel extract, which also served as a capping agent. Creation of AgNPs was confirmed using UV–visible spectroscopy, fluorescence emission spectroscopy, powder X-ray diffraction, and transmission electron microscopy, while size analysis was gathered from both transmission electron microscopy as well as dynamic light scattering. Analysis of all citrus peel extracts by gas chromatography–mass spectrometry indicated that the putative compounds responsible for successful AgNP synthesis with orange extract were aldehydes. The creation of AgNPs using environmentally benign reagents in minimal time paves the way for future studies on AgNP toxicity without risking interference from potentially toxic reagents and capping agents.

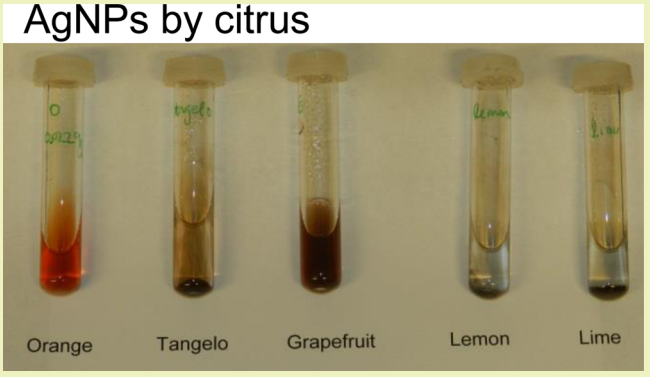

KEYWORDS: *Silver nanoparticles, Green chemistry, Microwave synthesis, Citrus peel*

INTRODUCTION

There has been much recent interest in using silver nanoparticles (AgNPs) in new technologies owing to their drastically enhanced properties over bulk silver, especially particles of diameters 30 nm and smaller.[1] These NPs are increasingly being incorporated into consumer products[2] despite rising evidence suggesting AgNPs have toxic effects on humans and experimental animal models meant to mimic human bio- and neurochemistry such as mice, rats, and *Drosophila*.[3−30] Many studies also suggest that AgNPs are quite harmful to the aquatic environment should they be inadvertently released into wastewater.[31−44] However, toxicity studies of this nature are often hindered by the AgNPs themselves used in the studies. In lieu of fast and convenient synthesis methods, many studies have utilized AgNPs, but the specification by which these materials have been synthesized and/or purified may not be included. Many current protocols for the synthesis of AgNPs utilize harsh and/or toxic chemicals.[45] The presence of these harsh synthetic conditions or contaminants may confound sensitive toxicity studies. Furthermore, AgNPs available for purchase are most often shipped as dry powders, and many studies fail to report the methods in which these AgNPs were redispersed in aqueous solutions.[46] The process of redispersion is quite crucial to the nature of the suspended AgNPs,[46,47] and inconsistencies in this methodology may also confound toxicity studies. As an alternative to purchased powders, the method for synthesizing AgNPs reported here was done so in a cost- and time-efficient manner and keeping with the principles of green chemistry.

The preparation of AgNPs using plant-based extracts[48] is widely growing in popularity; recently proposed syntheses use reagents such as many types of leaf extract,[49−54] including menthol,[55] aloe vera,[56] clove extract,[57] edible mushroom extract,[58] and extracts from coffees and teas.[59] AgNP synthesis using the extract of the navel orange (*Citrus sinensis*) was first proposed by Kaviya et al. in 2011.[60] AgNPs were both reduced from silver nitrate ($AgNO_3$) and capped by the compounds present in the orange peel extract.

Received: April 26, 2013
Revised: November 15, 2013

   dx.doi.org/10.1021/sc4003664 | *ACS Sustainable Chem. Eng.* XXXX, XXX, XXX–XXX

The objective of the work here was to use $AgNO_3$ and aqueous extracts of various citrus fruits (navel orange, ruby red grapefruit, Minneola tangelo, lemon, and lime) to prepare AgNPs in a microwave-assisted synthesis. It was hypothesized that the use of any citrus extract would lead to the successful synthesis of AgNPs. Use of the microwave allowed for improvement upon traditional heating to produce AgNPs while significantly reducing reaction time and thereby significantly improving experimental efficiency. Microwave parameters were first optimized using a Box–Benhken design for three factors. Upon successful synthesis and characterization of AgNPs using orange peel extract, other fruit (grapefruit, tangelo, lemon, and lime) extracts were evaluated as potential reagents for AgNP synthesis. Extracts were also analyzed by gas chromatography–mass spectrometry (GC/MS) to identify putative compounds in the extracts responsible for silver ion reduction.

Microwave heating holds many advantages over traditional heating-by-induction, though the reasons for this are currently debated.[61] Many of the benefits are as a result of the thermal capabilities introduced by microwave-assisted synthesis; microwaves rapidly achieve very high temperatures under a pressure-controlled environment.[61,62] As it has been reported that high temperatures accelerate the reductive properties of aldehydes,[63] this thermal effect may be responsible for the time efficiency of the synthesis presented here. Potential compounds in orange peel include citronellal, the compound responsible for oranges' distinct fragrance, and most likely one of the main reductive compounds present in orange peel extract. Other compounds responsible for reducing and capping include citrate, which is also a known reducing and capping agent,[45] and other compounds including limonene.

Microwave heating holds much promise in the regime of nanoparticle synthesis; the controlled high temperature enhances the nucleation process by which nanoparticles are initially created.[64] It has already been reported that as compared to traditional heating, microwave heating creates nanoparticles of higher degrees of crystallinity and narrower size distributions and grants greater control over the shape morphology of the nanostructures created.[62] Previous studies have also demonstrated that by using equivalent synthesis temperatures and times the microwave-assisted synthesis produced a far more robust reaction than traditional heat.[64] Indeed, there are a rapidly growing number of studies that show facile creation of nanoparticles using microwave heating,[62,64−72] and it is quickly becoming an attractive alternative in nanoparticle synthesis.

The nontoxic environmentally friendly synthesis proposed here produced AgNPs of an appropriately small size distribution using the extract of the peel of the common navel orange utilizing microwave-assisted synthesis in minimal time. It was determined that use of the other citrus extracts produced solutions that were dark gray and cloudy with a slight amber tint. By reporting the achievable method for synthesizing uniform AgNPs using orange peel extract, this work supports future studies aimed at investigating toxicity of these materials[73] without the confounding variable(s) of potentially toxic capping or reducing agents commonly used in other synthetic procedures.

MATERIALS AND METHODS

Chemicals and Reagents. Silver nitrate (ultrapure grade) and soluble starch were from Acros Organics (Thermo Fisher Scientific, Fairlawn, NJ). Acetone was purchased from Thermo Scientific (Asheville, NC). HPLC-grade methanol and methylene chloride were purchased from Fisher Scientific (Fairlawn, NJ). Navel oranges, ruby red grapefruit, Minneola tangelos, lemons, and limes were purchased from a local grocery store. Only HPLC-grade water (18 MΩ) from Barnstead E-pure system (Thermo Scientific, Asheville, NC) was used.

Preparation of Citrus Peel Extracts. Freshly prepared citrus peel extracts were prepared and used within two weeks of creation for all syntheses. Fruits were first rinsed thoroughly using DI water. Using a paring knife, segments of colored peel were carefully cut away from the fruit and then further cut into small pieces. Approximately 4 g of the citrus peel were quickly transposed to a 100 mL beaker containing approximately 40 mL of 18 MΩ H_2O to minimize evaporation of reagents. The mixture was then heated in a commercial food-grade microwave (Emerson, 700 W) for approximately 1 min, allowing the solution to boil for about 30 s. The mixture was filtered through Whatman no. 1 filter paper and then again through a 1.0 μm PTFE syringe filter (Nalgene, Thermo Scientific) to remove finer particulate. The aqueous extracts were then refrigerated for further use. These extracts were analyzed by GC/MS after sample preparation by solid phase extraction (SPE).

Synthesis of Silver Nanoparticles Using Citrus Peel Extracts. The laboratory-grade microwave synthesizer Discover SP (CEM Corporation, Matthews, NC) was used in all syntheses. Synthesis was carried out in CEM-supplied single-use 10 mL reaction vessels and septa designed for high temperature/pressure reactions in the microwave. Approximately 0.020 g of $AgNO_3$ (1.17×10^{-4} mol) was added to the vessel along with 1 mL of citrus peel extract, 5 mL of 18 MΩ H_2O, and a stir bar. The reagent-containing vessel was reacted in the CEM microwave at a temperature of 90 °C for 15 min with a maximum pressure of 15 psi.

Analysis of Citrus Peel Extracts by GC/MS. The sample was prepared for analysis by gas chromatography–mass spectrometry (GC/MS) analysis using SPE. Briefly, HyperSep Retain PEP SPE columns (Thermo Fisher Scientific, 3 mL volume/60 mg sorbent) were conditioned with a one-column volume of HPLC-grade methanol followed by a one-column volume of 18 MΩ DI water. For each fruit type, 10 mL of the citrus peel extract filtrate was loaded and allowed to elute by gravity. Finally, 10 mL of 18 MΩ DI water (as a reagent blank) was loaded onto a final SPE column. After elution, a vacuum (5 in Hg) was applied, and the columns were dried for 5 min. The retained compounds were eluted with 500 μL GC/MS-grade methylene chloride into test tubes containing approximately 500 mgof anhydrous sodium sulfate. Approximately 100 μL of methylene chloride extract was transferred to a polyspring glass insert of an amber glass autosampler vial prior to instrumental analysis.

GC/MS Instrumental Conditions. Samples were analyzed by GC/MS using a Hewlett-Packard 6890 plus gas chromatograph with 5975 mass selective detector. The column employed was a DB-5MS column (60 m, 0.20 mm i.d., 0.33 μm thickness; Agilent Technologies, Santa Clara, CA). Helium was used as the carrier gas at 1.0 mL/min. The initial column temperature was 45 °C (hold for 8 min) with a ramp of 10.0 °C/min to a final temperature of 300 °C (hold for 3 min), for a total run time of 35 min. A sample volume of 1.0 μL was injected at 250 °C in splitless mode. The MS detector was maintained at 280 °C, and electron ionization was utilized in the full scan mode from m/z 35–350 for positive ion detection. The solvent delay was 8 min.

Data comparison between the various citrus peel extracts and the sample blank was completed using AMDIS (Automated Mass Spectral Deconvolution and Identification System, version 2.68; http://chemdata.nist.gov/mass-spc/amdis/) with the NIST05 mass spectral library.

Silver Nanoparticle Characterization. *Centrifugation.* Centrifugation was performed in 45 mL tubes using a Fisher Scientific Marathon 22k centrifuge. Samples were first filtered through a 1.0 μm pore size TFF syringe filter (Whatman) to remove large particulate matter. Acetone was added to aqueous samples in a ratio of 1:2 to encourage precipitation of AgNPs. After allowing the AgNPs to precipitate, the samples were centrifuged for 10 min at 4500 rpm.

UV–Visible Spectroscopy. UV–vis spectra were collected in an optical-quality quartz cuvette with a 1 cm path length, requiring approximately 2 mL of solution to fill past the light path of the

instrument (Agilent 8453 system, Santa Clara, CA). Spectra were collected at room temperature (25 °C) using the appropriate aqueous citrus peel extracts as the blank, always taken with the same cuvette as used for analysis. Solutions were diluted immediately before analysis, if required, in order to normalize absorbance to approximately 2 AU. Spectra were collected from 300 to 700 nm.

Fluorescence Emission. All emission spectra were collected using a F-3010 fluorescence spectrophotometer (Hitachi, Pleasanton, CA) from a 3 mL optical-quality quartz cuvette from undiluted solutions. Both emission and excitation bandwidths were set to 10 nm. Printed paper graphs collected from this system were digitalized using PlotDigitizer software (Free Software Foundation; http://plotdigitizer.sourceforge.net/).

Dynamic Light Scattering (DLS) Analysis. All sizing DLS experiments were carried out on a ZetaPALS zeta potential analyzer (Brookhaven Instruments Corp., Holtsville, NY) using ZetaPlus particle sizing software, version 4.20, with a backscatter angle of 90° and a laser wavelength of 657.0 nm. Three milliliter disposable plastic-covered cuvettes were used for all sizing analysis, which were cleaned of dust using compressed air and loaded underneath a fume hood using a 0.2 μm syringe filter (Nalgene, Thermo Scientific) to minimize dust interference. Mean diameters reported were the mean of four measurements taken from at least four separate syntheses. Measurements were taken over 10 min, and means were computed by collecting at least seven runs of 10 1 min observations. Typical derived count rates were between 400 and 500 thousand counts per second (kcps). The viscosity of the medium used by the software in particle size calculation was 0.890 cP, and the temperature used was 25 °C.

Powder X-ray Diffraction. X-ray diffraction was performed on a Scintag X-2 advanced diffraction system (Cupertino, CA) equipped with Cu Kα radiation (λ = 1.54 Å) using a drop-cast sample of the AgNPs on a zero background Si plate sample holder (30 mm × 30 mm × 2.5 mm SiO_2 single crystal plate; MTI Corporation, Richmond, CA). AgNP samples were concentrated via centrifugation as described above prior to being drop-casted.

Transmission Electron Microscopy. Low-resolution transmission electron micrographs were obtained on a JEOL TEM 1400 (Peabody, MA) at a working voltage of 100 kV. TEM samples were prepared by dip-casting AgNPs dispersed in water onto carbon-coated copper TEM grids (200 mesh, Ted Pella) and were analyzed within minutes after preparation of the TEM grid. AgNP samples were concentrated via centrifugation as described above prior to being drop-casted. All sizing analysis performed using Adobe Photoshop CS3 software (Adobe Systems Inc., San Jose, CA).

Table 1. *P* Values from Main and Interactive Effects for Optimizing Microwave Synthesis Parameters Using Box–Benhken Design for Three Factors[a]

effect	*P* value	*F* value (*F* critical value)
main effects		
temperature	0.2406	1.6081 (3.8853)
pressure	0.7259	0.3291 (3.8853)
time	**0.0290**	4.8238 (3.8853)
interactive effects		
time × pressure	0.3193	1.5010 (4.1468)
time × temperature	**0.0199**	5.4482 (3.7870)
temperature × pressure	0.8893	0.3770 (3.7870)

[a]Significant *P* values are shown in bold.

RESULTS AND DISCUSSION

Optimization of Microwave Parameters. Microwave parameters were optimized using a Box–Benhken design for three factors (time, temperature, and pressure). Fifteen trials were completed with various combinations of time (1.5, 5, or 15 min), pressure limits (15, 17, or 20 psi), or temperature (75, 90, or 100 °C). Use of orange peel extract in the preparation of AgNPs had been previously described[60] and hence was used for the optimization of microwave reaction conditions. Samples were reacted using 1 mL of citrus peel extract (prepared as described above), approximately 0.020 mg of $AgNO_3$, and 5 mL of 18 MΩ water before analysis by UV–vis spectroscopy from 300 to 700 nm. Single-factor ANOVA was used to determine statistical significance (Table 1) of the

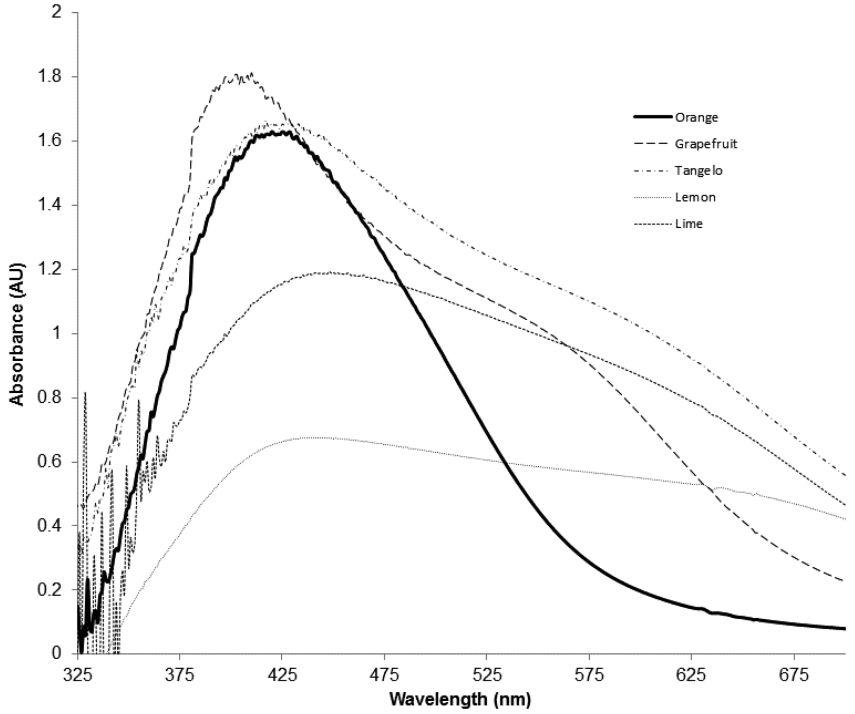

Figure 1. UV–vis absorbance spectrum of synthesized AgNPs from 325–700 nm is shown, with the absorbance maximum occurring at λ_{max} = 403 nm (grapefruit) and λ_{max} = 425 nm (orange and tangelo).

Table 2. Putative Compounds in Citrus Peel Extracts Prepared for GC/MS Analysis

no.	RT (min)	compound name	probability of ID	peak area[a]: orange	peak area: grapefruit	peak area: tangelo	peak area: lemon	peak area: lime	extract with max value
1	14.51	*n*-octanal	89.0	478635	–	–	–	–	**orange**
2	15.18	limonene	23.9	1568080	1436996	2992157	888819	1624755	tangelo
3	16.05	1-octanol	35.0	3651429	126258	105677	61041	747742	**orange**
4	16.67	3,7-dimethyl-1,6-octadien-3-ol (*β*-linalool)	65.9	3306807	468803	1761022	687795	1558844	**orange**
5	17.22	trans-*p*-mentha-2,8-dienal	59.6	138996	191533	–	–	18979	grapefruit
6	17.50	4-isopropenyl-1-methyl-2-cyclohexen-1-ol	44.1	1331	143203	–	38149	37212	grapefruit
7	17.98	1-nonanol	27.8	93849	–	–	3005	–	**orange**
8	18.32	*p*-menth-1-en-4-ol (4-Terpineol)	65.0	10926	12059	100173	326138	973563	lemon
9	18.56	*α*-Terpineol	48.6	3820887	571802	2334192	5981697	12107325	lemon
10	18.63	1S-*α*-pinene	11.0	100571	27245	–	–	128625	lime
11	18.95	3,7-dimethyl-6-octen-1-ol (*cis*-geraniol)	56.0	2501598	221242	512856	4067062	3547366	lemon
12	19.19	*β*-citral	71.1	1359539	149635	92081	6841315	22774833	lime
13	19.33	guariol (lemonol)	36.4	2029309	24847	40703	4195523	3156341	lemon
14	19.39	(R)-(-)-carvone	38.7	217241	179248	49449	132194	47064	**orange**
15	19.64	(E)-3,7-dimethyl-2,6-octadienal (*α*-citral)	72.8	1520670	223234	147931	10073986	18731869	lime
16	19.82	*p*-mentha-1,8-dien-3-one	88.4	48537	149409	325753	169334	885775	lime
17	19.94	perilla aldehyde	49.8	490599	196662	435668	250762	364586	**orange**
18	20.10	2-(4-methylenecyclohexyl)-2-propen-1-ol	54.6	976734	4815	210038	304668	62052	**orange**
19	20.25	perilla alcohol	68.0	330200	2491	259795	86505	76724	**orange**
20	20.33	2,6-dimethyl-2,6-octadiene-1,8-dial	24.8	64845	5045	35664	52884	41953	**orange**
21	20.41	2-ethyl-3-hydroxyhexyl-2-methylpropanoate	14.4	188428	2548	17757	8288	–	**orange**
22	20.92	4-isopropenyl-1-methyl-1,2-cyclohexanedial	83.9	234562	14153	21905	35214	37379	**orange**
23	20.99	eugenol	54.8	52202	17819	–	–	–	**orange**
24	21.03	8-hydroxylinalool	66.2	101557	13236	–	23567	10581	**orange**
25	22.17	2,6-dimethyl-7-octene-2,6-diol	15.2	66907	98027	170209	15947	180965	lemon
26	25.15	eudesm-7(11)-en-4-ol	31.4	87682	437580	–	183323	212083	grapefruit
27	25.45	(1-hydroxycyclohexyl)-phenylmethanone	86.8	44315	7497	–	–	–	**orange**
28	25.80	4-((1E)-3-hydroxy-1-propenyl)-2-methoxyphenol	72.2	42806	4772	7456	–	–	**orange**
29	26.21	tris(1-chloro-2-propyl) phosphate[b]	94.8	50922	32682	7175	42722	28948	**orange**
30	26.67	nootkatone	48.7	259100	8869070	257151	34786	185499	grapefruit
31	26.81	*β*-eudesmol	54.4	84435	345442	3099	2005	2566	grapefruit
32	29.47	thiabendazole[b]	95.7	240351	2512	541967	2424138	392249	lemon
33	30.01	imazalil[b]	94.0	64577	590478	263090	495214	–	grapefruit

[a]Total ion count (TIC) peak area for all reported peaks. [b]Indicates compounds that are xenobiotics (flame retardant and fungicides applied in the postharvest processing of citrus).

UV−vis data. All samples produced a λ_{max} of 402−428 nm and were a deep reddish-amber color, indicating the presence of AgNPs. Pressure limits had no statistically significant main or interactive effect. Time was both a statistically significant main effect (P = 0.0290) and interactive effect with temperature (P = 0.0199) with 15 min being the optimal time. Temperature was not a significant main effect and was therefore kept at 90 °C because of the higher UV−vis absorptivity compared to 75 °C. Therefore, for all other syntheses using citrus peel extracts, the reaction conditions were held at a pressure maximum of 15 psi for 15 min at 90 °C. Data concerning batch-to-batch variation for AgNPs synthesized for 15 min at various temperatures are included in Table S1 of the Supporting Information.

AgNP Characterization by UV−Vis. The use of any citrus peel extract in microwave-assisted synthesis of AgNPs was hypothesized to be an efficient way to synthesize and cap highly dispersed AgNPs. After allowing the reaction mixture to cool, the AgNP solution was subjected to optical studies. As shown in Figure 1, the synthesized AgNPs exhibited a broad absorbance at λ_{max} = 425 nm for AgNPs by orange and tangelo peel extract and λ_{max} = 403 nm for the grapefruit peel extract, owing to the surface plasmon resonance of the AgNPs.[74,75] This plasmon resonance is an intrinsic property of AgNPs and arises from the coupling between the electron cloud on the AgNP surface with the incident electromagnetic radiation[76−79] and typically occurs between 380 to 420 nm depending on the size of the AgNPs analyzed. The samples produced using lemon and lime extracts were very broad and required dilution prior to analysis because of the dark gray−black color of the tube contents after the microwave synthesis procedure. As shown in Figure 1, there was broad absorbance for all extracts but most notably for the lemon, lime, tangelo, and grapefruit extracts. The AgNPs by orange peel extract (dark black line, Figure 1) were most representative of what has been previously reported.[60]

dx.doi.org/10.1021/sc4003664 | ACS Sustainable Chem. Eng. XXXX, XXX, XXX−XXX

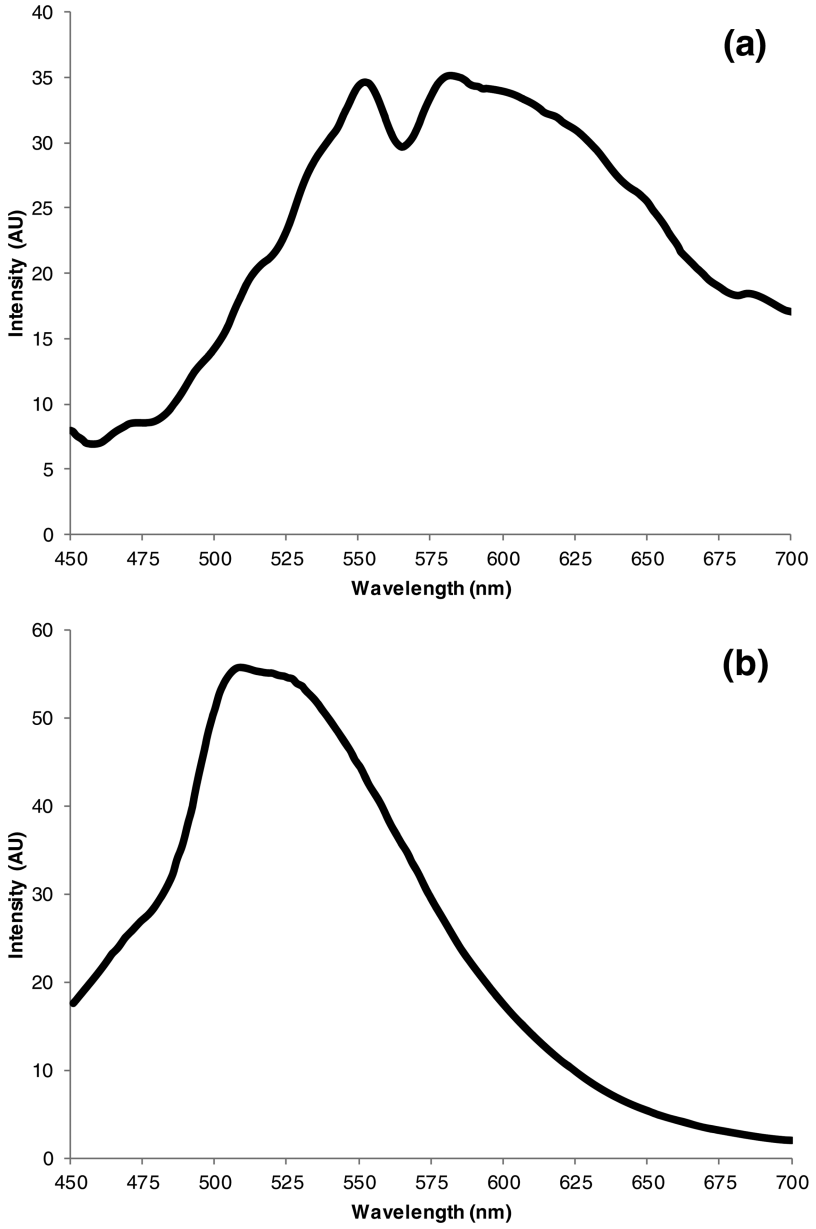

Figure 2. Fluorescence emission spectra where λ_{ex} = 430 nm of (a) AgNPs synthesized in orange peel extract and (b) orange peel extract alone. While orange peel extract strongly emits at λ_{em} = 510 nm, the synthesized AgNPs emit at λ_{em} = 551 and 582 nm.

The broad absorbance before and after the plasmon resonance peak (Figure 1) may likely result from multiple capping agents coming from varied natural compounds from orange peel extract present within the synthesis solution.[60] A blank of the orange peel extract treated to identical reactions conditions was used for comparison, and no significant absorbance was observed.

Comparison of Fruit Peel Extracts by GC/MS. Ten milliliters of the aqueous extracts used in the microwave-assisted synthesis were prepared for GC/MS analysis by SPE as described. Samples (1 μL) were injected, and the collected chromatograms and spectra were analyzed using AMDIS. The solvent peak (m/z 84) and column bleed peak (m/z 207) were excluded as ions from the deconvolution analyses. Upon completing a *simple* analysis for each data file, components in the spectra with a signal-to-noise ratio exceeding 40 were noted as being significant components. Given that the orange peel extract was successful in the synthesis of AgNPs, significant compounds in all other extracts (grapefruit, tangelo, lemon, and lime) were compared to the compounds identified in orange peel extract (Table 2).

Analytical standards for definitive identification of compounds were not used, and hence, the probability of correct identification is provided in Table 2. However, the presented results may be considered reasonable given the relative abundances of certain key compounds in given fruits. For example, the compound nootkatone (RT 26.67 min) is a sesquiterpene responsible for the aromatic nature of grapefruit;[80] this compound was found to be in highest abundance (~34 times higher than orange) in grapefruit when compared to other citrus extracts. As well, many of the compounds identified here, including limonene (RT 15.18 min), β-linalool (RT 16.67 min), α-terpineol (RT 18.56 min), and geraniol (RT 18.95 min), were previously identified as significant compounds in oranges.[81]

Briefly, several aldehydes were found to be only in the orange peel extract (n-octanal, retention time (RT) 14.51 min) or were

dx.doi.org/10.1021/sc4003664 | ACS Sustainable Chem. Eng. XXXX, XXX, XXX−XXX

found in higher abundance in the orange peel extract (perilla aldehyde, RT 19.94 min; 2,6-dimethyl-2,6-octadiene-1,8-dial, RT 20.33 min; and 4-isopropenyl-1-methyl-1,2-cyclohexanedial, RT 20.92 min). A number of alcohols were also found to be in higher abundance in orange peel: 1-octanol (RT 16.06 min), β-linalool (RT 16.67 min), 1-nonanol (17.98 min), 2-(4-methylenecyclohexyl)-2-propen-1-ol (RT 20.10 min), perilla alcohol (RT 20.25 min), and 8-hydroxylinalool (RT 21.03 min). Grapefruit and lime also contained significant levels of certain aldehydes, including *trans-p*-mentha-2,8-dienal, β-citral, and α-citral (Table 2). Chromatograms for all citrus extracts and the reagent blank are provided in Figures S1−S6 of the Supporting Information. The higher abundances of many aldehydes in the orange peel extract may be responsible for the improved AgNP synthesis by this extract.

Characterization of AgNPs Synthesized by Orange Peel Extract. The photoluminescence of the synthesized AgNPs by orange peel extract was also determined via fluorescence emissions spectroscopy (Figure 2). Owing to the fluorescence emission of the natural compounds present in the orange peel extract (Figure 2b) the spectrum was difficult to analyze; however, upon excitation at λ_{ex} = 430 nm, the synthesized AgNPs exhibited strong emission at λ_{em} = 551 nm and broadly at 582 nm (Figure 2a), which was not seen in the orange peel extract alone. Typical emissions reported in literature range anywhere from 465[82−84] to 550 nm[85,86] and vary drastically depending on the size of the AgNPs studied as well as their capping agents. AgNP photoluminescence has indeed been reported near and past 550 nm by several groups.[85−89] It has been reported that bulky capping agents cause a red-shift in the emissions spectra as compared to those capping agents that are less bulky.[82,86] As the natural compounds present in the orange peel extract may be somewhat bulky and very complex; this could serve to explain the red-shift seen in the emissions spectrum obtained as compared to other groups.

To confirm the presence of crystalline silver in the synthesized AgNPs by orange peel extract, X-ray diffraction (XRD) patterns were obtained (Figure 3). The peaks assigned to the diffraction pattern clearly show peaks corresponding to face-centered cubic (FCC) silver, with peaks at 2θ = 38.1°, 44.3°, 64.4°, 77.3°, and 81.5° corresponding to the (111), (200), (220), (311), and (222) planes, respectively. The AgNPs synthesized matched the NIST bulk silver reference (JCPDF 03-065-2871) as indicated by the green lines in Figure 3. Some extra peaks were noted that corresponded to citric acid hydrate (JCPDF 00-015-0985) that remained from synthesis, though some of the citric acid hydrate may also serve as a capping agent for the synthesized AgNPs. The broadness of the peaks indicated the small size of the AgNPs synthesized. The lattice constant "*a*" calculated from the AgNP samples using the instrument software was 4.08610 Å, which was in excellent agreement with the value reported in the literature for FCC silver (a = 4.086 Å, Joint Committee on Powder Diffraction Standards, file no. 04-0783). The AgNPs synthesized had no crystalline impurities other than the citric acid hydrate byproduct from synthesis.

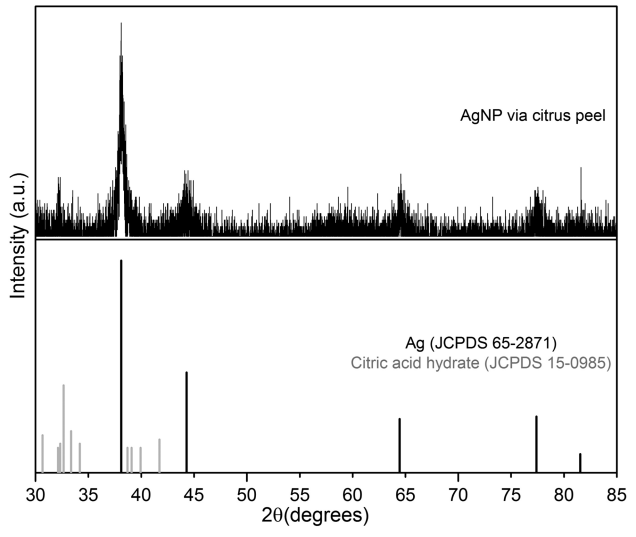

Figure 3. XRD pattern of synthesized AgNPs by orange peel extract. Gray lines indicate NIST bulk silver reference XRD (JCPDF 03-065-2871), and dark lines correspond with crystallized citric acid hydrate (JCPDF 00-015-0985).

Size Analysis of AgNPs by Orange Peel Extract. TEM revealed the formation of the AgNPs (Figure 4). The particles

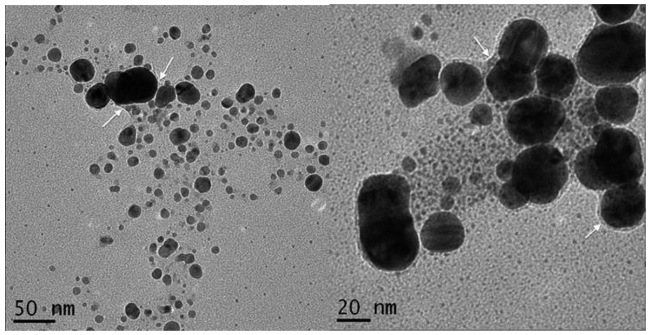

Figure 4. TEM images of AgNPs by orange peel extract at two magnification levels. White arrows indicate the presence of a thin organic layer surrounding the AgNPs.

were roughly spherical in shape and showed only a small degree of agglomeration. The TEM images showed what appears to be a layer of organic material surrounding the synthesized AgNPs and may explain the good dispersion in solution exhibited by these synthesized AgNPs. The AgNPs synthesized by this method were extremely small (Figure 4, right panel), though there were larger AgNPs synthesized by this method. While prominent in the TEM images, these larger diameter AgNPs were vastly outnumbered by those with smaller diameters in the TEM images analyzed (Figure 5). Optimizing reaction conditions for minimizing this size dispersion is one area of future research interest. While the largest AgNP size had a diameter of 56.1 nm, the mean size of the AgNPs as gathered from TEM images was 7.36 ± 8.06 nm (weighted mean ± standard deviation), with most particles (30.2%) residing between 2 and 4 nm. While many AgNPs were created with diameters over 10 nm, the vast majority (77.7%) had diameters of 10 nm or under, and 94.5% of particles were under 30 nm (Figure 5). Because NPs begin to exhibit nonbulk properties primarily at diameters of less than 20−30 nm,[1] the AgNPs synthesized here are well suited to support future research. DLS sizing data confirmed that the majority of AgNPs created were under 30 nm in diameter; however, due to the technique's tendency to overestimate particle size,[90] a mean diameter of 22.5 ± 2.4 nm was obtained (Figure 6). This large difference in AgNP diameters is of interest for future study, as is understanding the mechanisms that control NP size. Given the complexity of the orange peel extract

dx.doi.org/10.1021/sc4003664 | ACS Sustainable Chem. Eng. XXXX, XXX, XXX−XXX

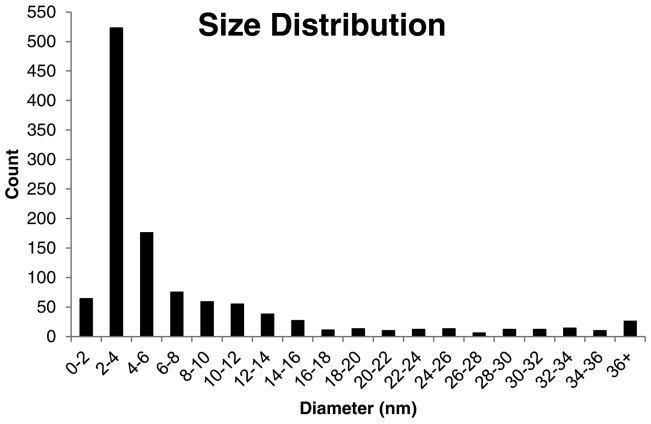

Figure 5. Size distribution of AgNPs by orange peel extract from TEM images.

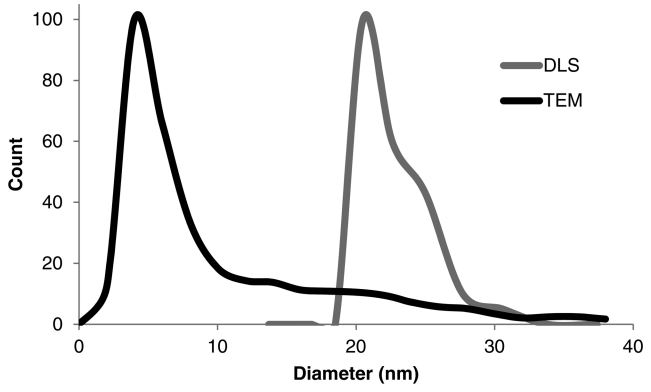

Figure 6. A comparison of DLS and TEM sizing analysis for the AgNPs synthesized.

utilized in the synthesis, the complexity of this matrix may have significant effects on agglomeration and deposition properties of the AgNPs.[40] As well, the effect of temperature on AgNP size in the citrus peel extract reaction matrix may be an important driver of NP size.[60]

AgNPs have been successfully synthesized utilizing microwave-assisted synthesis and orange peel extract as both a reducing and capping agent. The reduction of $AgNO_3$ and subsequent capping of AgNPs was thought to occur through the action of aldehyde-containing and other reducing compounds found in the orange peel extract (as described above), whereas the use of other citrus extracts to produce AgNPs was not as reliable. Future work will focus on the mechanism of aldehyde-assisted reduction of the Ag^+ to form AgNPs and which citrus-derived aldehyde is optimal for preparing AgNPs. Utilization of microwave-assisted synthesis produced nanoparticles with a smaller mean diameter determined via TEM versus DLS, while the elements present were confirmed from XRD patterns, UV−vis spectroscopy, and fluorescence emission data. The synthesized AgNPs were nearly spherical in shape and ran from under 1 nm in diameter to 56.1 nm, with an average size of 7.36 nm and a modal diameter of between 2 and 4 nm. The creation of AgNPs using environmentally benign reagents in minimal time paves the way for future studies on AgNP toxicity without risking interference from potentially toxic reagents and capping agents.

Safety Concerns. Solvents used (methanol, acetone, methylene chloride) should be used in a chemical fume hood and disposed of properly. Silver waste (from $AgNO_3$ and AgNP syntheses) should be disposed of properly.

■ ASSOCIATED CONTENT

Supporting Information

Data concerning batch-to-batch variation of synthesized AgNPs and chromatograms of citrus peel extracts (orange, tangelo, grapefruit, lemon, lime, and reagent blank). This material is available free of charge via the Internet at http://pubs.acs.org.

■ AUTHOR INFORMATION

Corresponding Author

*E-mail: jowens2@uccs.edu. Phone: (719) 255-3207. Fax: (719) 255-5205.

Present Address

§Genevieve A. Kahrilas: Department of Chemistry, Colorado State University, Ft. Collins, Colorado 80523, United States.

Notes

The authors declare no competing financial interest.

■ ACKNOWLEDGMENTS

Many thanks to CEM and Gordon Hall for provision of the synthesis-grade microwave. Special thanks to the UCCS Department of Physics and Vira Kravets for instrumentation time and assistance. Jacob Kershman is acknowledged for his review of the manuscript and for assistance in developing experiments. Students Jewell Anne Lee Hartman, Taylor Liptack, David Orban, and Shannon Seebeck are acknowledged for their assistance in AgNP synthesis and data collection. Faculty start-up funds and grants from the Committee on Research and Creative Works at the University of Colorado Colorado Springs to J. E. Owens are gratefully acknowledged. The helpful and perceptive comments of the reviewers are appreciated.

■ REFERENCES

(1) Auffan, M.; Rose, J.; Bottero, J.-Y.; Lowry, G. V.; Jolivet, J.-P.; Wiesner, M. R. Towards a definition of inorganic nanoparticles from an environmental, health and safety perspective. *Nat. Nanotechnol.* **2009**, *4*, 634−641, DOI: 10.1038/nnano.2009.242.

(2) Rejeski, D.; Kuiken, T.; Polischuk, P.; Pauwels, E. *Consumer Product Inventory*, 2012. The Project on Emerging Nanotechnologies. http://www.nanotechproject.org/cpi.

(3) Suresh, A. K.; Pelletier, D. A.; Wang, W.; Morrell-Falvey, J. L.; Gu, B.; Doklycz, M. J. Cytotoxicity induced by engineered silver nanocrystallites is dependent on surface coatings and cell types. *Langmuir* **2012**, *28*, 2727−2735, DOI: 10.1021/la2042058.

(4) Srivastava, M.; Singh, S.; Self, W. T. Exposure to silver nanoparticles inhibits selenoprotein synthesis and the activity of thioredoxin reductase. *Environ. Health Perspect.* **2011**, *120*, 56−61, DOI: 10.1289/ehp.1103928.

(5) Demir, E.; Vales, G.; Kaya, B.; Creus, A.; Marcos, R. Genotoxic analysis of silver nanoparticles in *Drosophila*. *Nanotoxicology* **2011**, *5*, 417−424, DOI: 10.3109/17435390.2010.529176.

(6) Wang, J.; Jensen, U. B.; Jensen, G. V.; Shipovskov, S.; Balakrishnan, V. S.; Otzen, D.; Pedersen, J. S.; Besenbacher, F.; Sutherland, D. S. Soft interactions of nanoparticles alter protein function and conformation in a size dependent manner. *Nano Lett.* **2011**, *11*, 4985−4991, DOI: 10.1021/nl202940k.

(7) Liu, Z.; Zhang, T.; Ren, G.; Yang, Z. Nano-Ag inhibiting action potential independent glutamatergic synaptic transmission but increasing excitability in rat CA1 pyramidal neurons. *Nanotoxicology* **2012**, *6*, 414−423, DOI: 10.3109/17435390.2011.583996.

(8) Zhao, C. M.; Wang, W. X. Importance of surface coatings and soluble silver in silver nanoparticles toxicity to *Daphnia magna*.

Nanotoxicology **2012**, *6*, 361−370, DOI: 10.3109/17435390.2011.579632.
(9) Maccormack, T. J.; Clark, R. J.; Dang, M. K.; Ma, G.; Kelly, J. A.; Veinot, J. G.; Goss, G. G. Inhibition of enzyme activity by nanomaterials: Potential mechanisms and implications for nanotoxicity testing. *Nanotoxicology* **2012**, *6*, 514−525, DOI: 10.3109/17435390.2011.587904.
(10) Sung, J. H.; Ji, J. H.; Song, K. S.; Lee, J. H.; Choi, K. H.; Lee, S. H.; Yu, I. J. Acute inhalation toxicity of silver nanoparticles. *Toxicol. Ind. Health* **2011**, *27*, 149−154, DOI: 10.1177/0748233710382540.
(11) Luther, E. M.; Koehler, Y.; Diendorf, J.; Epple, M.; Dringen, R. Accumulation of silver nanoparticles by cultured primary brain astrocytes. *Nanotechnol.* **2011**, *2011*, 37.
(12) El Badawy, A. M.; Silver, R. G.; Morris, B.; Scheckel, K. G.; Suidan, M. T.; Tolaymat, T. M. Surface charge-dependent toxicity of silver nanoparticles. *Environ. Sci. Technol.* **2011**, *45*, 283−287.
(13) Park, K.; Park, E. J.; Chun, I. K.; Choi, K.; Lee, S. H.; Yoon, J.; Lee, B. C. Bioavailability and toxicokinetics of citrate-coated silver nanoparticles in rats. *Arch. Pharm. Res.* **2011**, *34*, 153−158, DOI: 10.1007/s12272-011-0118-z.
(14) Zhao, C. M.; Wang, W. X. Comparison of acute and chronic toxicity of silver nanoparticles and silver nitrate to *Daphnia magna*. *Environ. Toxicol. Chem.* **2011**, *30*, 885−892, DOI: 10.1002/etc.451.
(15) Xu, L.; Takemura, T.; Xu, M.; Hanagata, N. Toxicity of silver nanoparticles as assessed by global gene expression analysis. *Mater. Express* **2011**, *1*, 74−79, DOI: 10.1166/mex2011.1010.
(16) Kim, S.; Kim, S.; Lee, S.; Kwon, B.; Choi, J.; Hyun, J. W.; Kim, S. Characterization of the effects of silver nanoparticles on liver cell using HR-MAS NMR spectroscopy. *Bull. Korean Chem. Soc.* **2011**, *32*, 2021−2026, DOI: 10.5012/bkcs.2011.32.6.2021.
(17) Warisnoicharoen, W.; Hongpiticharoen, P.; Lawanprasert, S. Alteration in enzymatic function of human cytochrome P450 by silver nanoparticles. *Res. J. Environ. Toxicol.* **2011**, *5*, 58−64, DOI: 10.3923/rjet.2011.58.64.
(18) Powers, C. M.; Badireddy, A. R.; Ryde, I. T.; Siedler, F. J.; Slotkin, T. A. Silver nanoparticles compromise neurodevelopment in PC12 cells: Critical contributions of silver ion, particle size, coating, and composition. *Environ. Health Perspect.* **2011**, *119*, 37−44, DOI: 10.1289/ehp.1002337.
(19) Bexiga, M. G.; Varela, J. A.; Wang, F.; Fenaroli, F.; Salvati, A.; Lynch, I.; Simpson, J. C.; Dawson, K. A. Cationic nanoparticles induce caspase 3-, 7- and 9-mediated cytotoxicity in a human astrocytoma cell line. *Nanotoxicology* **2011**, *5*, 557−567, DOI: 10.3109/17435390.2010.539713.
(20) Zook, J. M.; MacCuspie, R. I.; Locascio, L. E.; Halter, M. D.; Elliott, J. T. Stable nanoparticle aggregates/agglomerates of different sizes and the effect of their size on hemolytic cytotoxicity. *Nanotoxicology* **2011**, *5*, 517−530.
(21) Powers, C. M. Developmental Neurotoxicity of Silver and Silver Nanoparticles Modeled in Vitro and in Vivo. Ph.D. Dissertation, Duke University, 2010.
(22) Powers, C. M.; Wrench, N.; Ryde, I. T.; Smith, A. M.; Seidler, F. J.; Slotkin, T. A. Silver impairs neurodevelopment: Studies in PC12 cells. *Environ. Health Perspect.* **2010**, *118*, 73−79.
(23) Tang, J.; Xiong, L.; Zhou, G.; Wang, S.; Wang, J.; Liu, L.; Li, J.; Yuan, F.; Lu, S.; Wan, Z.; Chou, L.; Xi, T. Silver nanoparticles crossing through and distribution in the blood-brain barrier in vitro. *J. Nanosci. Nanotechnol.* **2010**, *10*, 6313−6317.
(24) Braydich-Stolle, L. K.; Lucas, B.; Schrand, A.; Murdock, R. C.; Lee, T.; Schlager, J. J.; Hussain, S. M.; Hofmann, M. C. Silver nanoparticles disrupt GDNF/Fyn kinase signaling in spermatogonial stem cells. *Toxicol. Sci.* **2010**, *116*, 577−589.
(25) AshaRani, P. V.; Mun, G. L. K.; Hande, M. P.; Valiyaveettil, S. Cytotoxicity and genotoxicity of silver nanoparticles in human cells. *ACS Nano* **2009**, *3*, 279−290, DOI: 10.1021/nn800596w.
(26) Sung, J. H.; Ji, J. H.; Park, J. D.; Yoon, J. U.; Kim, D. S.; Jeon, K. S.; Song, M. Y.; Jeong, J.; Han, B. S.; Han, J. H.; Chung, Y. H.; Chang, H. K.; Lee, J. H.; Cho, M. H.; Kelman, B. J.; Yu, I. J. Subchronic inhalation toxicity of silver nanoparticles. *Toxicol. Sci.* **2009**, *108*, 452−461, DOI: 10.1093/toxsci/kfn246.
(27) Kawata, K.; Osawa, M.; Okabe, S. In vitro toxicity of silver nanoparticles at noncytotoxic doses to HepG2 human hepatoma cells. *Environ. Sci. Technol.* **2009**, *43*, 6046−6051, DOI: 10.1021/es900754q.
(28) Kim, S.; Choi, J. E.; Choi, J.; Chung, K. H.; Park, K.; Yi, J.; Ryu, D. Y. Oxidative stress-dependent toxicity of silver nanoparticles in human hepatoma cells. *Toxicol. In Vitro* **2009**, *23*, 1076−1084.
(29) Foldbjerg, R.; Olesen, P.; Hougaard, M.; Dang, D. A.; Hoffmann, H. J.; Autrup, H. PVP-coated silver nanoparticles and silver ions induce reactive oxygen species, apoptosis and necrosis in THP-1 monocytes. *Toxicol. Lett.* **2009**, *190*, 156−162.
(30) Levard, C.; Hotze, E. M.; Lowry, G. V.; Brown, G. E., Jr. Environmental transformations of silver nanoparticles: Impact on stability and toxicity (critical review). *Environ. Sci. Technol.* **2012**, *46*, 6900−6914, DOI: 10.1021/es2037405.
(31) Shoults-Wilson, W. A.; Reinsch, B. C.; Tsyusko, O. V.; Bertsch, P. M.; Lowry, G. V.; Unrine, J. M. Effect of silver nanoparticle surface coating on bioaccumulation and reproductive toxicity in earthworms (*Eisenia fetida*). *Nanotoxicology* **2011**, *5*, 432−444.
(32) Coutris, C.; Hertel-Aas, T.; Lapied, E.; Joner, E. J.; Oughton, D. H. Bioavailability of cobalt and silver nanoparticles to the earthworm *Eisenia fetida*. *Nanotoxicology* **2012**, *6*, 186−195.
(33) Dimpka, C. O.; Calder, A.; Gajjar, P.; Merugu, S.; Huang, W.; Britt, D. W.; McLean, J. E.; Johnson, W. P.; Anderson, A. J. Interaction of silver nanoparticles with an environmentally beneficial bacterium, Pseudomonas chlororaphis. *J. Hazard. Mater.* **2011**, *188*, 428−435.
(34) Radniecki, T. S.; Stankus, D. P.; Neigh, A.; Nason, J. A.; Semprini, L. Influence of liberated silver from silver nanoparticles on nitrification inhibition of *Nitrosomonas europaea*. *Chemosphere* **2011**, *85*, 43−49.
(35) Fabrega, J.; Zhang, R.; Renshaw, J. C.; Liu, W. T.; Lead, J. R. Impact of silver nanoparticles on natural marine biofilm bacteria. *Chemosphere* **2011**, *85*, 961−966.
(36) Gubbins, E. J.; Batty, L. C.; Lead, J. R. Phytotoxicity of silver nanoparticles to *Lemna minor* L. *Environ. Pollut.* **2011**, *159*, 1551−1559.
(37) Turner, A.; Brice, D.; Brown, M. T. Interactions of silver nanoparticles with the marine microalga, Ulva lactuca. *Ecotoxicol.* **2012**, *21*, 148−154.
(38) Wise, J. P., Sr.; Goodale, B. C.; Wise, S. S.; Craig, G. A.; Pongan, A. F.; Walter, R. B.; Thompson, W. D.; Ng, A. K.; Aboueissa, A. M.; Mitani, H.; Spalding, M. J.; Mason, M. D. Silver nanospheres are cytotoxic and genotoxic to fish cells. *Aquat. Toxicol.* **2010**, *97*, 34−41.
(39) Lapied, E.; Moudilou, E.; Exbrayat, J. M.; Oughton, D. H.; Joner, E. J. Silver nanoparticle exposure causes apoptotic response in the earthworm *Lumbricus terrestris* (Oligochaeta). *Nanomedicine* **2010**, *5*, 975−984.
(40) Navarro, E.; Baun, A.; Behra, R.; Hartmann, N. B.; Filser, J.; Miao, A. J.; Quigg, A.; Santschi, P. H.; Sigg, L. Environmental behavior and ecotoxicity of engineered nanoparticles to algae, plants, and fungi. *Ecotoxicol.* **2008**, *17*, 372−386.
(41) Navarro, E.; Piccapietra, F.; Wagner, B.; Marconi, F.; Kaegi, R.; Odzak, N.; Sigg, L.; Behra, R. Toxicity of silver nanoparticles to *Chlamydomonas reinhardtii*. *Environ. Sci. Technol.* **2008**, *42*, 8959−8964, DOI: 10.1021/es801785m.
(42) Yin, L.; Cheng, Y.; Espinasse, B.; Colman, B. P.; Auffan, M.; Wiesner, M. R.; Rose, J.; Liu, J.; Bernhardt, E. S. More than the Ions: The effects of silver nanoparticles on *Lolium multiflorum*. *Environ. Sci. Technol.* **2011**, *45*, 2360−2367.
(43) Bilberg, K.; Hovgaard, M. B.; Besenbacher, F.; Baatrup, E. In vivo toxicity of silver nanoparticles and silver ions in zebrafish (*Danio rerio*). *J. Toxicol.* **2012**, *2012*, DOI:10.1155/2012/293784.
(44) Ringwood, A. H.; McCarthy, M.; Bates, T. C.; Carroll, D. L. The effects of silver nanoparticles on oyster embryos. *Mar. Environ. Res.* **2010**, *69* (Suppl), S49−51.
(45) Tolaymat, T. M.; El Badawy, A. M.; Genaidy, A.; Scheckel, K. G.; Luxton, T. P.; Suidan, M. T. An evidence-based environmental perspective of manufactured silver nanoparticle in syntheses and

applications: A systematic review and critical appraisal of peer-reviewed scientific papers. *Sci. Total Environ.* **2010**, *408*, 999−1006.
(46) Taurozzi, J. S.; Hackley, V. A.; Wiesner, M. R. Ultrasonic dispersion of nanoparticles for environmental, health and safety assessment - Issues and recommendations. *Nanotoxicology* **2010**, *5*, 711−729.
(47) Taurozzi, J. S.; Hackley, V. A.; Wiesner, M. R. *Reporting Guidelines for the Preparation of Aqueous Nanoparticle Dispersions from Dry Materials*; NIST Special Publication 1200-1; National Institute of Standards and Technology: Gaithersburg, MD, 2012.
(48) Hebbalalu, D.; Lalley, J.; Nadagouda, M. N.; Varma, R. S. Greener techniques for the synthesis of silver nanoparticles using plant extracts, enzymes, bacteria, biodegradable polymers, and microwaves. *ACS Sustainable Chem. Eng.* **2013**, *1* (7), 703−712, DOI: 10.1021/sc4000362.
(49) Kouvaris, P.; Delimitis, A.; Zaspalis, V.; Papadoupoulous, D.; Tsipas, S. A.; Michailidis, N. Green synthesis and characterization of silver nanoparticles produced using *Arbutus Unedo* leaf extract. *Mater. Lett.* **2012**, *76*, 18−20.
(50) Kaviya, S.; Santhanalakshmi, J.; Viswanathan, B. Green synthesis of silver nanoparticles using *Polyalthia longifolia* leaf extract along with D-sorbitol: Study of antibacterial activity. *J. Nanotechnol.* **2011**, *2011*, DOI:10.1155/2011/152970.
(51) Jha, A. K.; Prasad, K.; Kumar, V.; Prasad, K. Biosynthesis of silver nanoparticles using Eclipta leaf. *Biotechnol. Prog.* **2009**, *25*, 1476−1479.
(52) Jha, A. K.; Prasad, K.; Prasad, K.; Kulkarni, A. R. Plant system: nature's nanofactory. *Colloids Surf., B* **2009**, *73*, 219−223.
(53) Huang, J.; Li, Q.; Sun, D.; Lu, Y.; Su, Y.; Yang, X.; Wang, H.; Wang, Y.; Shao, W.; He, N.; Hong, J.; Chen, C. Biosynthesis of silver and gold nanoparticles by novel sundried *Cinnamomum camphora* leaf. *Nanotechnol.* **2007**, *18*, DOI:10.1088/0957-4484/18/10/105104.
(54) Leela, A.; Vivekanandan, M. Tapping the unexploited plant resources for the synthesis of silver nanoparticles. *African J. Biotechnol.* **2008**, *7*, 3162−3165.
(55) Mubarak Ali, D.; Thajuddin, N.; Jeganathan, K.; Gunasekaran, M. Plant extract mediated synthesis of silver and gold nanoparticles and its antibacterial activity against clinically isolated pathogens. *Colloids Surf., B* **2011**, *85*, 360−365.
(56) Chandran, S. P.; Chaudhary, M.; Pasricha, R.; Ahmad, A.; Sastry, M. Synthesis of gold nanotriangles and silver nanoparticles using Aloe vera plant extract. *Biotechnol. Prog.* **2006**, *22*, 577−583.
(57) Vijayaraghavan, K.; Kamala Nalini, S. P.; Udaya Prakash, N.; Madhankumar, D. Biomimetic synthesis of silver nanoparticles by aqueous extract of *Syzygium aromaticum*. *Mater. Lett.* **2012**, *75*, 33−35.
(58) Philip, D. Biosynthesis of Au, Ag, and Au-Ag nanoparticles using edible mushroom extract. *Spectrochim. Acta, Part A* **2009**, *73*, 374−381.
(59) Nadagouda, M. N.; Varma, R. S. Green synthesis of silver and palladium nanoparticles at room temperature using coffee and tea extract. *Green Chem.* **2008**, *10*, 859−862.
(60) Kaviya, S.; Santhanalakshmi, J.; Viswanathan, B.; Muthumary, J.; Srinivasan, K. Biosynthesis of silver nanoparticles using *Citrus sinensis* peel extract and its antibacterial activity. *Spectrochim. Acta, Part A* **2011**, *79*, 594−598.
(61) Galema, S. A. Microwave chemistry. *Chem. Soc. Rev.* **1997**, *26*, 233−238.
(62) Tsuji, M.; Hashimoto, M.; Nishizawa, Y.; Kubokawa, M.; Tsuji, T. Microwave-assisted synthesis of metallic nanostructures in solution. *Chemistry* **2005**, *11*, 440−452.
(63) Nath, S.; Ghosh, S. K.; Panigrahi, S.; Pal, T. Aldehyde assisted wet chemical route to synthesize gold nanoparticles. *Indian J. Chem. A* **2004**, *43*, 1147−1151.
(64) Jiang, H.; Moon, K.-s.; Zhang, Z.; Pothukuchi, S.; Wong, C. P. Variable frequency microwave synthesis of silver nanoparticles. *J. Nanopart. Res.* **2006**, *8*, 117−124.
(65) Sato, S.; Mori, K.; Ariyada, O.; Atsushi, H.; Yonezawa, T. Synthesis of nanoparticles of silver and platinum by microwave-induced plasma in liquid. *Surf. Coat. Technol.* **2011**, *206*, 955−958.
(66) Bahadur, N. M.; Furusawa, T.; Sato, M.; Kurayama, F.; Siddiquey, I. A.; Suzuki, N. Fast and facile synthesis of silica coated silver nanoparticles by microwave irradiation. *J. Colloid Interface Sci.* **2011**, *355*, 312−320.
(67) Dwivedi, R.; Maurya, A.; Verma, A.; Prasad, R.; Bartwal, K. S. Microwave assisted sol-gel synthesis of tetragonal zirconia nanoparticles. *J. Alloys Compd.* **2011**, *509*, 6848−6851.
(68) Blosi, M.; Albonetti, S.; Dondi, M.; Martelli, C.; Baldi, G. Microwave-assisted polyol synthesis of Cu nanoparticles. *J. Nanopart. Res.* **2011**, *13*, 127−138.
(69) Marquardt, D.; Vollmer, C.; Thomann, R.; Steurer, P.; Mulhaupt, R.; Redel, E.; Janiak, C. The use of microwave irradiation for the easy synthesis of graphene-supported transition metal nanoparticles in ionic liquids. *Carbon* **2011**, *49*, 1326−1332.
(70) Horikoshi, S.; Abe, H.; Torigoe, K.; Abe, M.; Serpone, N. Access to small size distributions of nanoparticles by microwave-assisted synthesis. Formation of Ag nanoparticles in aqueous carboxymethylcellulose solutions in batch and continuous-flow reactors. *Nanoscale* **2010**, *2*, 1441−1447.
(71) Pal, A.; Shah, S.; Devi, S. Microwave-assisted synthesis of silver nanoparticles using ethanol as a reducing agent. *Mater. Chem. Phys.* **2009**, *114*, 530−532.
(72) Hu, B.; Wang, S.-B.; Wang, K.; Zhang, M.; Yu, S.-H. Microwave-assisted rapid facile "green" synthesis of uniform silver nanoparticles: Self-assembly into multilayered films and their optical properties. *J. Phys. Chem. C* **2008**, *112*, 11169−11174.
(73) Baruwati, B.; Simmons, S. O.; Varma, R. S.; Veronesi, B. "Green" synthesized and coated nanosilver alters the membrane permeability of barrier (intestinal, brain endothelial) cells and stimulates oxidative stress pathways in neurons. *ACS Sustainable Chem. Eng.* **2013**, *a* (7), 753−759, DOI: 10.1021/sc400024a.
(74) Khan, M. A. M.; Kumar, S.; Ahamed, M.; Alrokayan, S. A.; Alsalhi, M. S.; Alhoshan, M.; Aldwayyan, A. S. Structural and spectroscopic studies of thin film of silver nanoparticles. *Appl. Surf. Sci.* **2011**, *257*, 10607−10612.
(75) Kim, T.-G.; Kim, Y. W.; Kim, J. S.; Park, B. Silver-nanoparticle dispersion from the consolidation of Ag-attached silica colloid. *J. Mater. Res.* **2004**, *19*, 1400−1407.
(76) Bohren, C. F.; Huffman, D. R. *Absorption and Scattering of Light by Small Particles*; Wiley: New York, 1983.
(77) Link, S.; El-Sayed, M. A. Optical properties and ultrafast dynamics of metallic nanocrystals. *Annu. Rev. Phys. Chem.* **2003**, *54*, 331−366.
(78) Kreibig, U.; Vollmer, M. *Optical Properties of Metal Clusters*; Springer-Verlag: New York, 1995.
(79) Kerker, M. The optics of colloidal silver: Something old and something new. *J. Colloid Interface Sci.* **1985**, *105*, 297−314.
(80) Shaw, P. E.; Wilson, C. W., III Importance of nootkatone to the aroma of grapefruit oil and the flavor of grapefruit juice. *J. Agric. Food Chem.* **1981**, *29*, 677−679.
(81) Dharmawan, J.; Kasapis, S.; Sriramula, P.; Lear, M. J.; Curran, P. Evaluation of aroma-active compounds in Pontianak orange peel oil (*Citrus nobilis* Lour. Var. *microcarpa Hassk.*) by gas chromatography−olfactometry, aroma reconstitution, and omission test. *J. Agric. Food Chem.* **2009**, *57*, 239−244.
(82) Alqudami, A.; Annapoorni, S. Fluorescence from metallic silver and iron nanoparticles prepared by exploding wire technique. *Plasmonics* **2007**, *2*, 5−13.
(83) Yeshchenko, O. A.; Dmitruk, I. M.; Alexeenko, A. A.; Losytskyy, M. Y.; Kotko, A. V.; Pinchuk, A. O. Size-dependent surface-plasmon-enhanced photoluminescence from silver nanoparticles embedded in silica. *Phys. Rev. B* **2009**, *79*, 235438.
(84) Jiang, Z.; Yuan, W.; Pan, H. Luminescence effect of silver nanoparticle in water phase. *Spectrochim. Acta, Part A* **2005**, *51*, 2488−2494.
(85) El-Shishtaway, R. M.; Asiri, A. M.; Al-Otaibi, M. M. Synthesis and spectroscopic studies of stable aqueous dispersion of silver nanoparticles. *Spectrochim. Acta, Part A* **2011**, *79*, 1505−1510.

(86) Vigneshwaran, N.; Nachane, R. P.; Balasubramanya, R. H.; Varadarajan, P. V. A novel one-pot 'green' synthesis of stable silver nanoparticles using soluble starch. *Carbohydr. Res.* **2006**, *341*, 2012−2018.
(87) Duran, N.; Marcato, P. D.; Alves, O. L.; De Souza, G. I. H.; Esposito, E. Mechanistic aspects of biosynthesis of silver nanoparticles by several *Fusarium oxysporum* strains. *J. Nanobiotechnol.* **2005**, *3*, DOI:10.1186/1477-3155-3-8.
(88) Zhao, Y.; Jiang, Y.; Fang, Y. Spectroscopy property of Ag nanoparticles. *Spectrochim. Acta, Part A* **2006**, *65*, 1003−1006.
(89) Vigneshwaran, N.; Ashtaputre, N. M.; Varadarajan, P. V.; Nachane, R. P.; Paralikar, K. M.; Balasubramanya, R. H. Biological synthesis of silver nanoparticles using the fungus *Aspergillus flavus*. *Mater. Lett.* **2007**, *61*, 1413−1418.
(90) MacCuspie, R. I.; Rogers, K.; Patra, M.; Suo, Z.; Allen, A. J.; Martin, M. N.; Hackley, V. A. Challenges for physical characterization of silver nanoparticles under pristine and environmentally relevant conditions. *J. Environ. Monit.* **2011**, *13*, 1212−1226.